# An Integrative Simulation Approach to Weight Reduction in Poly(ethylene terephthalate) Bottles

**Fugen Daver,[1] Bilal Demirel,[2] Jeffrey Sutanto,[1] Chao Wei Pang[1]**

[1]*School of Aerospace, Mechanical and Manufacturing Engineering, RMIT University, Bundoora, Victoria 3083, Australia*
[2]*Department of Metallurgy and Materials Engineering, Bartin University, Bartin, Turkey*

Received 19 December 2010; accepted 10 January 2012
DOI 10.1002/app.36780
Published online in Wiley Online Library (wileyonlinelibrary.com).

**ABSTRACT:** Poly(ethylene terephthalate) (PET) is a widely used resin in the production of carbonated soft drink (CSD) bottles produced by injection-stretch blow molding. A reduction in the bottle weight brings down the cost of packaging by reducing the materials and manufacturing costs. This article presents an integrative simulation study where 1.5-L CSD bottles produced from preforms with different weights were assessed in terms of process viability and product quality. The simulation results were analyzed with respect to the experimental data obtained for the currently used CSD bottle made from 40 g of preform. We found that we could reduce the weight of the PET bottles by 7.5% without jeopardizing the functionality of the bottles in terms of the structural performance properties, such as the top-load and burst strengths.  J. Appl. Polym. Sci. 000: 000–000, 2012

**Key words:** injection molding; mechanical properties; processing; structure–property relations; simulations

## INTRODUCTION

Food-grade poly(ethylene terephthalate) (PET) resin is one of the most commonly used packaging materials because of its excellent mechanical and physical properties. With the introduction of the injection-stretch blow-molding (ISBM) technique in the early 1970s, it was possible to maximize the beneficial properties of PET resin, and the use of PET in bottle manufacturing has shown a steep increase since then. The global PET market in 2009 was 15.3 million tons, and it is expected to grow at a compound annual growth rate of 4.9% until 2020. Carbonated soft drinks (CSDs) and bottled water account for more than 65% of the global PET demand.[1] Given the amount of PET resin used for CSD and bottled water, even a small reduction in bottle weight makes a significant contribution toward reducing the cost of plastics packaging.

PET bottles are usually produced in either one-stage or two-stage ISBM machines. The process starts with the injection molding of a tubelike preform. The preform is stretched axially by a stretch rod and radially by pressurized air until it takes on the shape of the bottle mold. During the blow stage, a preblow is applied to prevent the axial stretch rod from contacting the inside of the preform, as this may result in defects in the bottle. When the rod reaches the bottom of the container, a high blow pressure is applied to impart the intricate details of the bottle mold and to improve the cooling efficiency. In the two-stage ISBM process, injection-molded preforms are stored until subsequent blow molding, usually at the bottle filling stage. Hence, the preforms require reheating, whereas in the single-stage ISBM process, the injection-molded preforms are shaped into bottles once the preform temperature is just above its glass-transition temperature without reheating.[2] During the ISBM process, PET molecules undergo biaxial orientation and associated strain hardening. The biaxial orientation of PET molecules directly influences the mechanical and barrier properties of the bottles.[3,4] Strain hardening, which is temperature and strain rate dependent, provides a self-leveling effect on the stretching preform; this is important in achieving a uniform wall thickness. Therefore, control of process conditions together with the preform design provides a means of achieving the required bottle quality.

There have been various simulation studies that have optimized the preform shape and process conditions. Such modeling studies, which are performed with both extrusion blow and stretch blow molding, are mainly motivated by a reduction in part development time, a reduction in tooling cost, and an improvement in part quality. One recent simulation study demonstrated a new design approach to predict the optimal preform geometry and optimal operating conditions for stretch blow molding.[5] The

*Correspondence to:* F. Daver (fugen.daver@rmit.edu.au).

numerical approach combines a constrained, gradient-based optimization algorithm that iterates automatically over predictive finite element software. Strategy allows one to target a specified container thickness distribution by consecutively manipulating the preform geometry in terms of both the thickness and the shape. In another simulation study of stretch blow molding, the finite element optimization method was developed to determine the optimal thickness profile of a preform for a blow-molded part for a required wall thickness distribution.[6] Likewise, in extrusion blow molding, a closed-loop optimization approach analogous to a classical process control system to manipulate the process parameters to obtain the required thickness distribution in the final blown part is employed.[7] In another example, soft computing techniques are used for the extrusion blow-molding process to ensure product quality and to reduce manufacturing costs. The process optimization objective is to obtain a uniform thickness of blown parts; and the design optimization objective is to minimize the part weight subject to stress concentration.[8]

In the integrative simulation study presented here, we aimed to reduce the PET resin used in CSD packaging by reducing the preform weight in a systematic manner. The ISBM process simulation of the bottles was followed by a virtual structural analysis to assess the performance of the PET bottles. The preforms with different weights were virtually stretch-blown into 1.5-L CSD bottles by means of the commercial simulation software BlowView version 8.4 (National Research Council of Canada, Boucherville, Canada). The resultant thickness profile of the bottles and the microstructure-dependent material properties were input into ANSYS finite element software to assess the top-load and burst strengths of the bottles. Although there were other properties, such as $CO_2$ barrier resistance, that were also of importance for the CSD bottles, we focused only on the structural performance of the bottles. The gas-barrier properties of the bottles will be the topic of a subsequent study.

## EXPERIMENTAL

### Materials used

The PET resin used for the simulation studies was chosen from the database of the BlowView 8.4 simulation software. It was Eastman PET 9921 bottle-grade PET manufactured by Eastman Chemical Co. (Kingsport, TN), with an intrinsic viscosity of 0.80 dL/g.

### BlowView 8.4 simulation software

The BlowView 8.4 plastic blow-molding software, which was developed by the National Research Council of Canada, simulates and optimizes the blow-molding processes.[9] The software focuses on three processes: (1) extrusion blow molding, (2) stretch blow molding, and (3) thermoforming. It helps to predict how blow-molded parts will perform before one commits to expensive tool manufacturing. The software solves the nonisothermal solid mechanics constitutive equations specifically for the individual phases of the blow-molding process. It incorporates thermomechanical material models: viscoelastic models for polyolefins and viscohyperelastic material models for PET. We successfully used the software to redesign the 1.5-L CSD bottle base.[10,11]

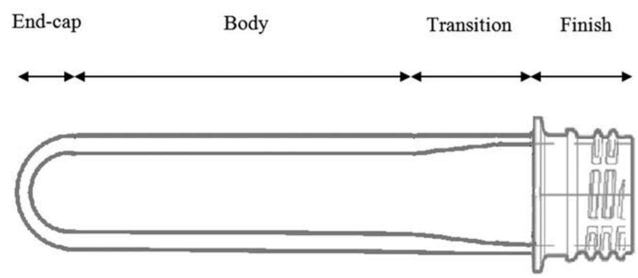


**Figure 1** Preform design.

### ISBM process simulation via BlowView 8.4

The bottle mold and stretch rod profiles were modeled in CATIA software and were imported into the BlowView 8.4 simulation software, whereas the preform model was designed with the BlowView 8.4 software tools. For each of the seven preforms, a preform design with different wall thicknesses was considered.

#### Preform design

The preform that was used in this simulation study could be divided into four sections: finish (threaded end), transition, body, and end cap (Fig. 1). The transition section was further divided into two zones.

For the purpose of this simulation experiment, the current finish (PCO 1810) was used, and its weight was kept constant at 5.1 g for all of the preforms. The thickness ratio between the end cap and the body of the current 40 g of preform was used to reduce the wall thickness of the preform across the transition zones and the body. The preform transition zone and the body section were shaped like a cylinder but with different diameters at each end [Fig. 2(a)]. Therefore, a typical section volume ($x$), which was representative of the body and the transition zones of the preform, was calculated by the subtraction of the outside frustum from the inner frustum as follows:

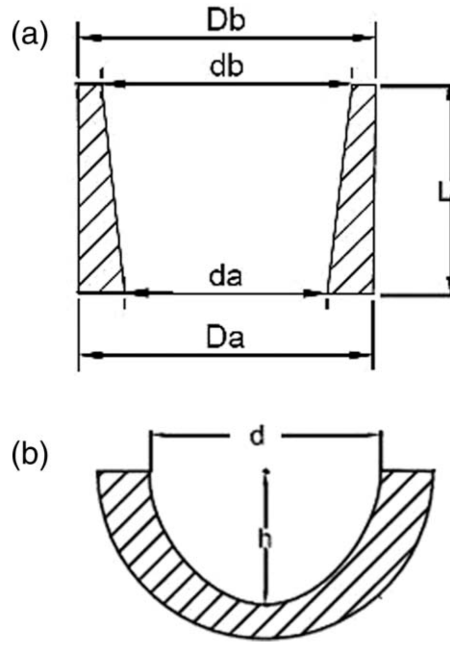


**Figure 2** Preform design of the (a) body and transition zones (b) end cap.

$$x = \left[\frac{\pi L_a}{12}\left(D_a^2 + D_a D_b + D_b^2\right)\right] - \left[\frac{\pi L_a}{12}\left(d_a^2 + d_a d_b + d_b^2\right)\right] \quad (1)$$

where $L_a$ is the length of the frustum, $D_a$ and $D_b$ are the outer frustum diameters, and $d_a$ and $d_b$ are the inner frustum diameters.

The end cap of the preform is shown in Figure 2(b). The end-cap volume was calculated by the subtraction of an elliptical cone from a half-sphere as follows:

$$\text{End} - \text{cap volume} = \left(\frac{1}{2} \times \frac{\pi d^3}{6}\right) - \left(\frac{\pi d^2 h}{6}\right) \quad (2)$$

where $d$ and $h$ are the diameter and height of the elliptical cone, respectively.

The resultant preform weight was found by the addition of the end cap, body, and transition weights together with the fixed weight of the thread [Eq. (3)]:

$$\text{Preform weight} = [(V_a + V_b + V_c + V_{\text{Endcap}}) \times \rho + \text{Thread}] \quad (3)$$

where $V_a$ is the volume of body; $V_b$ and $V_c$ are the volumes of transition zones; $V_{\text{end-cap}}$ is the volume of end-cap of the perform; ρ is the density of PET.

Seven different preforms, from 37 g up to 40 g with 0.5 g increments, were generated in this manner. The preform weight was reduced down to 37 g; further reductions in weight resulted in perform blowouts or sticking effects, where the perform stuck to the stretch rod during the simulation process and prevented successful bottle production.

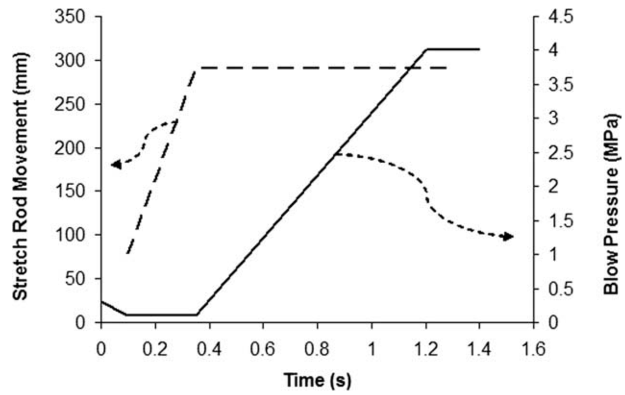


**Figure 3** ISBM process conditions.

Process conditions

Figure 3 shows the ISBM process conditions employed in the simulation of the bottles with different preform weights. The pressure was kept at 0.1 MPa for 0.35 s; then, it was gradually increased up to 4 MPa in 0.85 s, and finally, it was maintained at 4 MPa for 0.2 s. The stretch rod speed was taken to be 0.84 m/s; hence, it reached the bottle base within 0.26 s.

Figure 4 shows the temperature profile on the preform. Preform temperature is 93°C at the end-cap section, increasing up to 110°C along the preform body, until it joins the thread which is at 50°C.

### ANSYS finite element simulation software

The ANSYS simulation software was developed by ANSYS, Inc., a leading simulation software company. The ANSYS structural module addresses the unique concerns of pure structural simulations. It offers nonlinear structural capabilities and linear capabilities to deliver high-quality, reliable structural

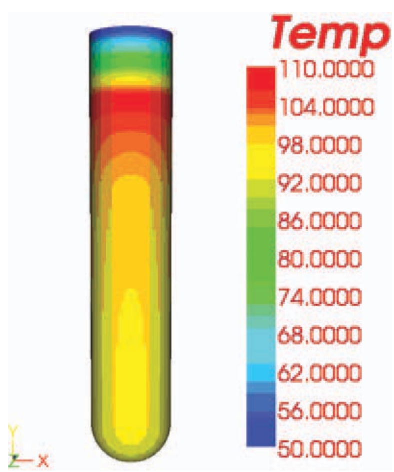


**Figure 4** Preform temperature profile used in the simulation. [Color figure can be viewed in the online issue, which is available at wileyonlinelibrary.com.]

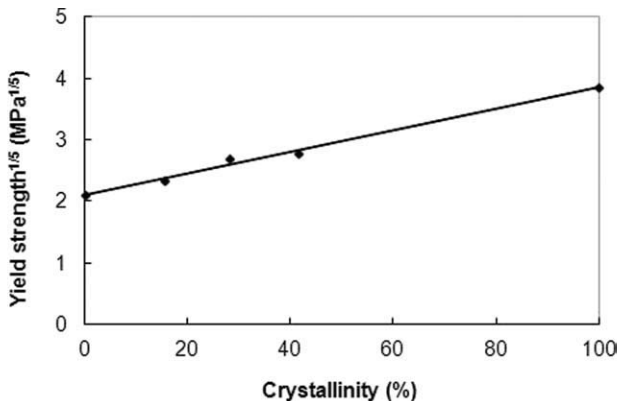


**Figure 5** Crystallinity dependence of the yield strength for PET at 263 K.

simulation results. The software is capable of reading the output files generated by BlowView simulation software for structural analysis.

### Von Mises stresses

When a body is subjected to internal or external forces, a three-dimensional stress is generated. Hence, there are three principal stresses acting along the $x$, $y$, and $z$ dimensions when a bottle is under top-load forces or internal pressures. Even though none of the principal stresses exceeds the yield stress of the material, an equivalent stress, which is called the *von Mises stress* may exceed the yield stress of the material; hence, this equivalent stress can bring the bottle to failure. In this study, we simulated the von Mises stress distribution on the whole bottle and recorded the maximum stress and maximum displacement for each top-load and internal pressure loading. The structural performances of the bottles with different preform weights were then compared on the basis of their maximum von Mises stresses.

### Simulation of the top-load and burst strength of the PET bottles via ANSYS

The ISBM process simulation of the PET bottles with different preform weights was carried out with the BlowView 8.4 software. The resulting thickness profile of each PET bottle was exported into the ANSYS structural module to assess the top-load and burst strengths of the lightweight bottles. The top-load strength assesses the overall durability of the bottles necessary for the filling and stacking of the bottles during manufacturing, storage, and distribution. The burst strength provides an assessment of the overall stability of the bottle under the carbonation pressure of the contents; it is equal to the pressure at which the bottle would burst. The burst strength is particularly important in bottles intended for carbonated beverages to ensure that the bottles do not blow up during the filling stage and that the filled bottles do not expand excessively during storage and/or the pasteurization process. To assess the performance of the bottles in terms of the top-load strength and burst strength, bottle deformation was simulated under (1) a top-load force and (2) internal pressure for all of the bottles with different preform weights. Instead of using a constant value to define the material properties, we used microstructure-dependent mechanical performance models to calculate typical mechanical properties, including the Young's modulus, yield, and maximum stress or impact resistance.[12]

In Eq. (4), Young's modulus at room temperature ($E_o$) is given as a function of the polymer crystallinity ($\chi$) and the level of molecular orientation, as measured by the average birefringence:[13]

$$E_o = \left(\left[(1-\chi)\sqrt[5]{E_{\mathrm{am}}} + \chi\sqrt[5]{E_c}\right]\right)^5 \exp(c\Delta_{\mathrm{av}}) \quad (4)$$

where $E_c$ and $E_{\mathrm{am}}$ are the modulus values of the perfectly crystalline and perfectly amorphous materials, respectively; $c$ is the material constant, given as 1.59, and $\Delta_{\mathrm{av}}$ is the average birefringence of the two phases. The Young's modulus of the perfectly crystalline and totally amorphous PET materials were obtained directly from the literature.[14] The yield strength values of the totally crystalline and totally amorphous PETs were derived according to the two-phase model based on experimental data provided at 263 K.[15] As shown in Figure 5, a straight line was fitted between the crystallinity and the yield strength values. After the extrapolation of this straight line, the yield strength values were derived as 40.9 and 857.6 MPa for the totally amorphous and the totally crystalline PET, respectively. Table I gives the model fit results of the crystallinity dependence of the modulus and yield strength of PET.

The crystallinity and birefringence values for all bottles with different preform weights were obtained by the BlowView simulation software along the arc of each bottle. These values were then input into the relevant equations to obtain local, microstructure-dependent elastic modulus and yield strength values, as shown in Figures 6 and 7, respectively.

**TABLE I**
**Model Fits of the Crystallinity Dependence of the Modulus and Yield Strength of PET**

| | Elastic modulus (MPa) | Yield strength (MPa) |
|---|---|---|
| Amorphous PET (100%) | 1745.3 | 40.9 |
| Crystalline PET (100%) | 8569.7 | 857.6 |

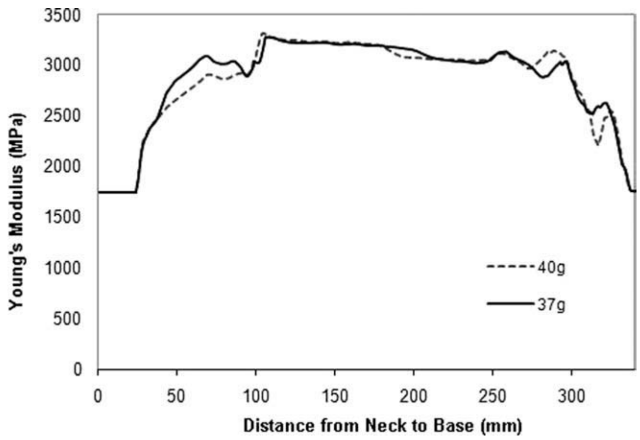


**Figure 6** Elastic modulus along the arc of the bottle (from the neck to the base).

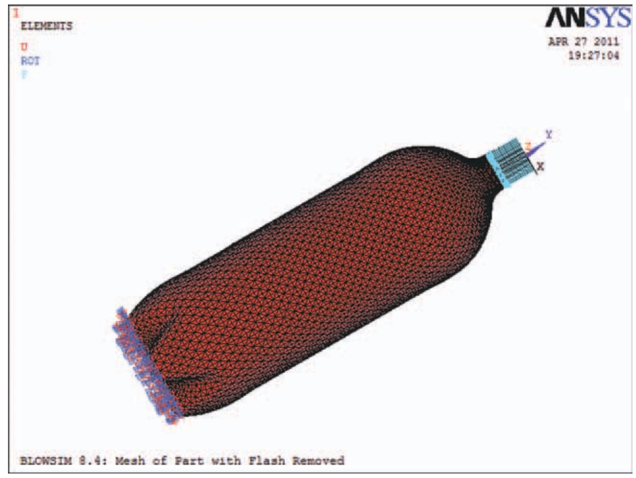


**Figure 8** Application of constraints on the base and loads on the bottle top. [Color figure can be viewed in the online issue, which is available at wileyonlinelibrary.com.]

In the simulation of the top-load strength of the bottles via ANSYS, the bottle was constrained on the bottle base, and the load was applied on the top of the bottle (Fig. 8). After the application of a range of loads between 200 and 300 N on the top of the bottle, the maximum von Mises stresses and maximum deformation values were recorded for each bottle.

Similarly, in the simulation of the burst strength of the bottles, the top section of the bottle was clamped, and internal pressure was applied on the inner surfaces of the bottle (Fig. 9). The maximum von Mises stresses and the maximum deformation values were recorded for each bottle under a range of internal pressures between 1.0 and 1.5 MPa.

## RESULTS AND DISCUSSION

### Thickness profiles of the bottles

Thickness profiles were obtained for all PET bottles with different preform weights between 37 and 40 g. However, for the sake of clarity, thickness profiles are given for only the lightest and heaviest bottles (i.e., 37 and 40 g of preforms) in Figure 10. The bottle base thickness was found to be 3.24 mm for the heaviest bottle (40 g of preform), whereas it was 2.85 mm for the lightest bottle (37 g of preform). The bottle base became thinner as the weight of the preform was reduced.

### Top-load and burst strength values of the bottles

The maximum von Mises stresses and displacement values were plotted at the application of a 200-N top-load force for all of the bottles (Fig. 11). As the preform weight decreased, the maximum von Mises stress and displacement increased. Although the 40-g preform design, which is currently in use, resulted in a higher top-load strength, the maximum stress observed in the bottle was not a lot different compared to the other preform designs of lower

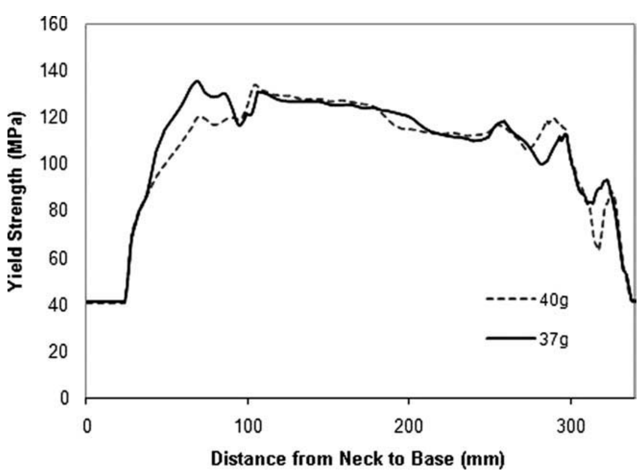


**Figure 7** Yield strength along the arc of the bottle (from the neck to the base).

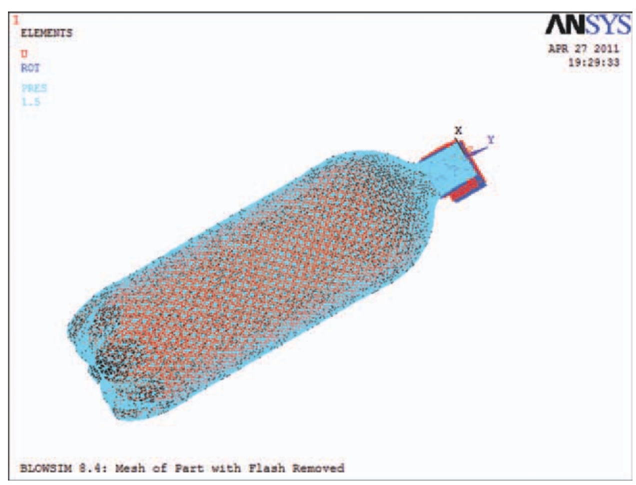


**Figure 9** Application of clamps on the bottle top and internal pressure. [Color figure can be viewed in the online issue, which is available at wileyonlinelibrary.com.]

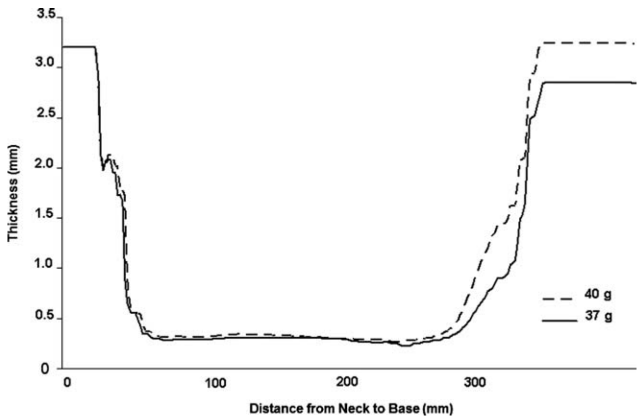


**Figure 10** Thickness profiles of the bottles (37 and 40 g of preforms).

weight. The difference between the heaviest bottle (40 g of preform) and the lightest bottle (37 g of preform) was rather small. With the application of 200-N top loads, the maximum displacement differed by 7 μm, which was insignificant, and the maximum stress differed only by 200 kPa between the heaviest and the lightest bottles.

Similarly, Figure 12 shows the maximum von Mises stresses and maximum displacement values at 1 MPa of pressure on the inner surfaces of the bottles with different preform weights. As the preform weight decreased, the maximum stress and maximum displacement increased. The maximum stress and maximum displacement values obtained for the lightweight bottles were much lower than those of the current 40-g preform bottle. The difference between the heaviest bottle (40 g of preform) and the lightest bottle (37 g of preform) was significant: at 1 MPa of internal pressure, the difference in the maximum displacement was about 0.1 mm, and the difference in maximum stresses was about 4 MPa between the heaviest and the lightest bottles.

## Comparison of the experimental top-load strength with the simulation

According to the local manufacturers of CSD bottles, the minimum top-load strength requirement for

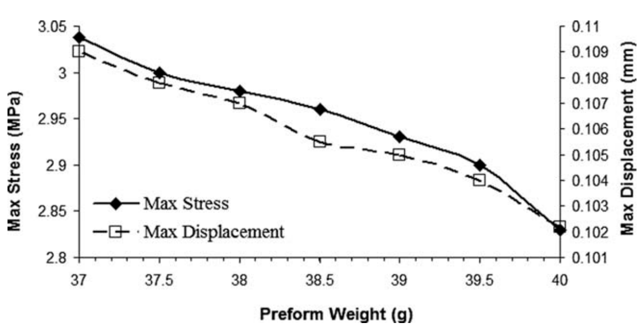


**Figure 11** Maximum stress and displacement of the bottles under a 200-N top load.

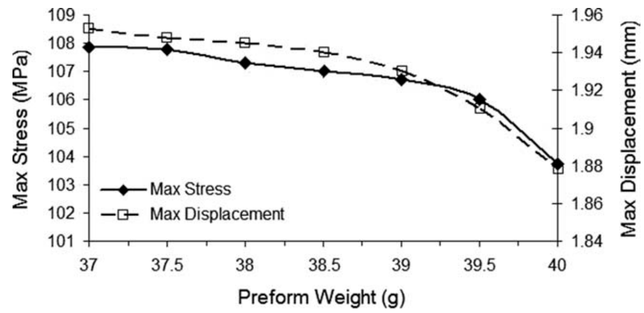


**Figure 12** Maximum stress and displacement of bottles at an internal pressure of 1.0 MPa.

1.5-L CSD bottles is 196 N; this corresponds to a compression force equal to the weight of approximately 15 bottles filled up with water. Therefore, in this study, the minimum requirement for the top-load strength of the bottles was set at 200 N. The simulation results shown in Figure 11 were analyzed with respect to the actual top-load strength of a 1.5-L CSD bottle (40 g of preform), which was found to be 307 N.[11]

The maximum von Mises stress reached 3.038 MPa when the lightest bottle (37 g of preform) was simulated under a a 200-N top load. Although this stress was higher for the lighter bottles, nevertheless, it was still much lower than the 4.344-MPa critical stress recorded for the heaviest bottle (40 g of preform) under the actual buckling load of 307 N. On the basis of this comparative analysis, all of the lightweight bottles considered in this study were expected to pass the minimum 200-N top-load strength requirement without buckling.

## Comparison of the experimental burst strength with the simulation

According to the local manufacturers of CSD bottles, the minimum burst strength requirement for the 1.5-L CSD bottles was 0.95 MPa; this was well above the internal carbonation pressure of 0.4–0.6 MPa recorded for such bottles. Hence, in this study, the minimum requirement for the burst strength of the bottles was set at 1 MPa. The simulation results shown in Figure 12 were analyzed with respect to the actual burst strength of the 1.5-L CSD bottle (40 g of preform), which was found to be 1.4 MPa.[11]

When the lightest bottle (37 g of preform) was simulated under an internal pressure of 1 MPa, the maximum von Mises stress reached 107.8 MPa. Although for a given top-loading condition, the maximum stress was higher for lighter bottles, this stress was still well below the critical value of 145.2 MPa recorded for the heaviest bottle (40 g) under the actual burst strength of 1.4 MPa. On the basis of this comparative analysis, all of the lightweight bottles considered in this study were expected to pass the 1-MPa minimum burst strength requirement of the packaging industry.

## CONCLUSIONS

PET bottles are widely used in CSD packaging applications. Any reduction in the amount of PET material used for CSD bottles could save materials and manufacturing costs. In this study, BlowView simulation software was used to simulate the stretch blow molding of seven preform models with different weights. The simulation results in terms of bottle thickness profiles and microstructure-dependent elastic modulus and yield strength values were then exported into ANSYS software for top-load and burst strength analysis. As the preform weight decreased, the bottle base became thinner. Although the reduction in preform weight resulted in lower thickness, particularly in the base of the bottles, the lightweight bottles still performed as well as the current bottles with 40 g of preform. The simulation results show that the lighter bottles (down to 37 g) were able to fulfill industry requirements in terms of the top-load and burst strengths. Further studies are required to analyze the lightweight bottles in terms of other important parameters, in particular, the gas permeability of the bottles, which is relevant to the CSD packaging industry. This will be the subject of a future investigation.

### References


1. Chemicals Market Research Reports. http://www.reportsandreports.com/cat/chemicals-market-research.html (accessed Dec 2010).
2. Blow Moulding Handbook: Technology, Performance, Markets, Economics—The Complete Blow Molding Operation; Rosato, D. V., Rosato, D. V., Eds.; Hanser: Munich, 1989.
3. PET Packaging Technology; Brooks, D. W., Giles, G. A., Eds.; Wiley-Blackwell: New York, 2002.
4. Liu, R. Y. F.; Hu, Y. S.; Schrialdi, D. A.; Hiltner, A.; Baer, E. J Appl Polym Sci 2004, 94, 671.
5. Thibault, F.; Malo, A.; Lanctot, B.; Diraddo, R. Polym Eng Sci 2007, 47, 289.
6. Lee, D. K.; Soh, S. K. Polym Eng Sci 1996, 36, 1513.
7. García-Rejón, A.Advances in Blow Molding Process Optimisation; Rapra Technology: Shropshire, United Kingdom, 1994.
8. Yu, J. C.; Hung, T. R.; Juang, J. Y.; Thibault, F. J Intell Manufacturing 2004, 15, 625.
9. BlowView. http://www.pacesimulations.com/download/brochures/BlowView.pdf (accessed February 2011).
10. Demirel, B.; Daver, F. J Appl Polym Sci 2009, 114, 1126.
11. Demirel, B.; Daver, F. J Appl Polym Sci 2009, 114, 3811.
12. Handbook of Polymer Science and Technology; Cheremisinoff, N. P., Ed.; Marcel Dekker: New York, 1989; Vol. 2.
13. Patterson, D.; Ward, I. M. Trans Faraday Soc 1957, 53, 1516.
14. Laroche, D.; DiRaddo, R.; Brace, J. Proc Soc Plast Eng Annu Tech Conf 2001, 1, 117.
15. Fernandez, J. O.; Swallowe, G. M. J Mater Sci 2000, 35, 4405.